J|A|C|S
ARTICLES
Published on Web 12/08/2005

8-Hydroxyquinoline Derivatives as Fluorescent Sensors for Magnesium in Living Cells

Giovanna Farruggia,*,† Stefano Iotti,*,‡ Luca Prodi,*,§ Marco Montalti,§ Nelsi Zaccheroni,§ Paul B. Savage,*,|| Valentina Trapani,⊥ Patrizio Sale,⊥,× and Federica I. Wolf*,⊥

Contribution from the Dipartimento di Biochimica "G. Moruzzi", Via Irnerio 48, e Dipartimento di Chimica "G. Ciamician", Via Selmi 2, Università degli Studi di Bologna, 40126 Bologna, Italy, Dipartimento di Medicina Clinica e Biotecnologia Applicata "D. Campanacci", Universita' di Bologna, Via Massarenti, 9, 40138 Bologna, Italy, Department of Chemistry and Biochemistry, Brigham Young University, Provo, Utah, and Istituto di Patologia Generale e Centro di Ricerche Oncologiche Giovanni XXIII, Università Cattolica del Sacro Cuore, Roma, Largo F. Vito 1, 00168 Roma, Italy

Received September 22, 2005; E-mail: giovanna.farruggia@unibo.it; stefano.iotti@unibo.it; luca.prodi@unibo.it; paul_savage@byu.edu; fwolf@rm.unicatt.it

Abstract: Despite the key role of magnesium in many fundamental biological processes, knowledge about its intracellular regulation is still scarce, due to the lack of appropriate detection methods. Here, we report the spectroscopic and photochemical characterization of two diaza-18-crown-6 hydroxyquinoline derivatives (DCHQ) and we propose their application in total Mg^{2+} assessment and in confocal imaging as effective Mg^{2+} indicators. DCHQ derivatives **1** and **2** bind Mg^{2+} with much higher affinity than other available probes (K_d = 44 and 73 μM, respectively) and show a strong fluorescence increase upon binding. Remarkably, fluorescence output is not significantly affected by other divalent cations, most importantly Ca^{2+}, or by pH changes within the physiological range. Evidence is provided on the use of fluorometric data to derive total cellular Mg^{2+} content, which is consistent with atomic absorption data. Furthermore, we show that DCHQ compounds can be effectively employed to map intracellular ion distribution and movements in live cells by confocal microscopy. A clear staining pattern consistent with known affinities of Mg^{2+} for biological ligands is shown; moreover, changes in the fluorescence signal could be tracked following stimuli known to modify intracellular Mg^{2+} concentration. These findings suggest that DCHQ derivatives may serve as new tools for the study of Mg^{2+} regulation, allowing sensitive and straightforward detection of both static and dynamic signals.

Introduction

Magnesium ion, the most abundant divalent cation in cells, is required for many cell processes such as proliferation[1] and cell death.[2] It is involved in the regulation of hundreds of enzymes and molecules of different structure and function.[3] Most ATP in cells is bound to Mg^{2+} since $MgATP^{2-}$ is the active species in enzyme binding and the energy-producing form in active transport[4] and muscular contraction.[5] Thus, alteration in total or free magnesium can have significant consequences for cell metabolism and cell functions.

Although the biochemistry of Mg^{2+} has been thoroughly studied in vitro, a full understanding of cellular magnesium homeostasis has not been achieved. Cytosolic Mg^{2+} concentration is regulated by plasma membrane and organelle transport and by intracellular binding. It is maintained far from electrochemical equilibrium by means of inward and outward transport mechanisms.[6] Cytosolic free Mg^{2+} levels are reported to be 0.2−1 mM depending on the tissue and/or the measurement techniques employed,[7] representing less than 10% of the total

† Dipartimento di Biochimica "G. Moruzzi", Università degli Studi di Bologna.
‡ Departimento di Medicina Clinica e Biotecnologia Applicata "D. Campanacci" Università degli Studi di Bologna.
§ Dipartimento di Chimica "G. Ciamician", Università degli Studi di Bologna.
|| Brigham Young University.
⊥ Università Cattolica del Sacro Cuore.
× Present address: IRCCS San Raffaele, Via della Pisana 235, 00163 Roma, Italy.

(1) (a) Wolf, F. I.; Cittadini, A. *Front. Biosci.* **1999**, *4*, 607−617. (b) Rubin, H. *BioEssays* **2005**, *27*, 311−320.
(2) Eskes, R.; Antonsson, B.; Osen Sand, A.; Montessuit, R.; Richter, C.; Sadoul, R.; Mazzei, G.; Nichols, A.; Martinou, J. C. *J. Cell Biol.* **1998**, *143*, 217−224.
(3) *Magnesium and the Cell*; Birch, N. J., Ed.; Academic Press: San Diego, CA, 1993.
(4) (a) Ramirez, F.; Marecek, J. F. *Biochim. Biophys. Acta* **1980**, *589*, 21−29. (b) Kuby, S. A.; Noltman, E. A. In *The Enzymes*, 2nd ed.; Boyer, P. D., Ed., Academic Press: New York, 1959; Vol. 6, pp 515−603. (c) Repke, K. R. H. *Ann. N.Y. Acad. Sci.* **1982**, *402*, 272−286.
(5) Wells, J. A.; Knoeber, C.; Sheldon, M. C.; Werber, M. M.; Yount, R. G. *J. Biol. Chem.* **1980**, *255*, 11135−11140.
(6) (a) Romani, A.; Scarpa, A. *Front. Biosci.* **2000**, *5*, 720−734. (b) Schmitz, C.; Perraud, A.-L.; Johnson, C. O.; Inabe, K.; Smith, M. K.; Penner, R.; Kurosaki, T.; Fleig, A.; Scharenberg, A. M. *Cell* **2003**, *114*, 91−200. (c) Wolf, F. I. *Sci. STKE* **2004**, *233*, 23.

10.1021/ja056523u CCC: $33.50

Mg^{2+}; the remainder is bound or sequestered in different cellular organelles.

It has been presumed that cellular magnesium, in particular the free form, is kept constant at the level necessary for cellular metabolic demands and that, under physiological conditions, its concentration does not undergo drastic and rapid changes. In recent years, however, it has been demonstrated that sizable fluxes of Mg^{2+} can cross the plasma membrane in either direction following hormonal and nonhormonal stimuli, resulting in major changes in total and, to a lesser extent, free Mg^{2+} content (see ref 8 for review). Furthermore, in vivo NMR measurements have shown that concentrations of free Mg^{2+} change in human skeletal muscle under different metabolic conditions and that these changes can only partially be ascribed to redistribution of Mg^{2+} among the different equilibria within the cytosolic milieu.[7g,h,9]

In this context, the need for a sensitive and reliable tool to measure concentrations and fluctuations of cellular Mg^{2+} becomes very stringent, since available techniques have serious limitations. Atomic absorption spectroscopy is very sensitive and accurate but requires volatilization of the sample and a relatively high number of cells, and it does not discriminate between free and bound forms. On the other hand, in vivo NMR spectroscopy allows an accurate measurement of cytosolic free Mg^{2+} but supplies no information on the total Mg^{2+} concentration and its distribution among cellular subcompartments. Electron probe microanalysis has been exploited to measure Mg^{2+} content in distinct cellular subcompartments in freeze-dried cryosections. This technique again does not provide information on free and bound Mg^{2+} and does not allow kinetic measurements of Mg^{2+} fluxes.[10]

Fluorescent probes, if properly designed, can offer a suitable solution. They are widely used to evaluate changes in intracellular metal ion concentrations. In particular, their application in fluorescence confocal imaging allows dynamic measurements of cellular content and distribution of the targeted ion, giving a means of mapping the concentration of an analyte in a sample. The available fluorescent probes for intracellular magnesium are mainly derived from those designed for calcium (mag-fura, mag-indo, mag-fluo, etc.),[11] but despite the chemical modifications to increase their selectivity toward Mg^{2+}, they retain cross-reactivity with Ca^{2+} and dependence on pH. In addition, these Mg^{2+}-specific fluorophores are characterized by a K_d in the millimolar range, which is appropriate to measure mainly the free fraction of cellular Mg^{2+}. In fact, cytosolic free Mg^{2+} concentrations are in the range of 10^{-4} M, while total cellular Mg^{2+} is up to 100-fold higher. Increasing evidence shows that fluctuations of free intracellular Mg^{2+} concentrations are modest compared to massive changes of total cellular Mg^{2+};[12] thus, modifications of Mg^{2+} availability to influence different biological functions are thought to be accomplished by substantial modifications of the distribution of total Mg^{2+} among cellular subcompartments. In this scenario, a tool able to detect and/or discriminate between free and total Mg^{2+} and between Mg^{2+} content of cytosolic and intracellular subcompartments would be particularly useful. Recently, a new family of Mg-binding fluorescent probes named KMGs has been designed, and their application to the study of intracellular Mg^{2+} homeostasis seems promising.[13]

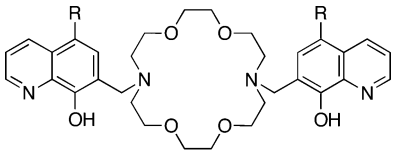

1 R = H
2 R = Cl

Figure 1. Chemical structures of DCHQ fluorescent probes **1** and **2**.

The synthesis and photophysical studies have recently been reported of a new class of fluorescent sensors for Mg^{2+} ion based on diaza-18-crown-6 appended with two hydroxyquinoline groups (DCHQ) bearing different substituents.[14,15] These molecules have been proposed as effective chemosensors for different ions; in particular, some members of this family demonstrated high specificity for Mg^{2+} with negligible interference by Ca^{2+}.[15] In this study we focused our attention on the two molecules shown in Figure 1. We studied their spectroscopic characteristics, selectivity, sensitivity, and affinity for Mg^{2+} in aqueous solution and their possible utilization as intracellular chemosensors of Mg^{2+} by confocal fluorescence microscopy.

Experimental Section

General Spectroscopic Methods. All reagents were purchased from Sigma and were Ultrapure grade. Dulbecco's phosphate-buffered saline (DPBS) without Ca^{2+} and Mg^{2+} (8 g/L NaCl, 0.20 g/L KCl, 0.20 g/L Na_2HPO_4, and 0.20 g/L KH_2PO_4, pH 7.2) was prepared in doubly distilled water. A 1 M solution of $MgSO_4$ was prepared, and concentration accuracy was checked by atomic absorption spectroscopy. The fluorescent probes were dissolved in dimethyl sulfoxide (DMSO) at a concentration of 1 mg/mL (**1**, 1.7 mM; **2**, 1.5 mM), and aliquots were kept at 4 °C in the dark.

UV−Visible Spectroscopy. Absorption spectra were recorded on a Uvikon (Kontron) or a Perkin-Elmer λ 40 spectrophotometer.

Fluorescence Spectroscopy. Fluorescence spectra (450 W Xe lamp), excited-state lifetimes (pulsed laser at 406 nm), and steady-state and

(7) (a) Taylor, J. S.; Vigneron, D. B.; Murphy-Boesch, J.; Nelson, S. J.; Kessler, H. B.; Coia, L.; Curran, W.; Brown, T. R. *Proc. Natl. Acad. Sci. U.S.A.* **1991**, *88*, 6810−6814. (b) Halvorson, H. R.; Vande Linde, A. M. Q.; Helpern, J. A.; Welch, M. A. *NMR Biomed.* **1992**, *5*, 53−58. (c) Barker, P. B.; Butterworth, E. J.; Boska, M. D.; Nelson, J.; Welch, K. M. A. *Magn. Reson. Med.* **1999**, *41*, 400−406. (d) Iotti, S.; Frassineti, C.; Alderighi, L.; Sabatini, A.; Vacca, A.; Barbiroli, B. *NMR Biomed.* **1996**, *9*, 24−32. (e) Ward, K. M.; Rajan, S. S.; Wysong, M.; Radulovic, D.; Clauw, D. J. *Magn. Reson. Med.* **1996**, *36*, 475−480. (f) Irish, A. B.; Thompson, C. H.; Kemp, G. J.; Taylor, D. J.; Radda, G. K. *Nephron* **1997**, *76*, 20−25. (g) Iotti, S.; Frassineti, C.; Alderighi, L.; Sabatini, A.; Vacca, A.; Barbiroli, B. *Magn. Reson. Imaging* **2000**, *18*, 607−614. (h) Iotti, S.; Frassineti, C.; Sabatini, A.; Vacca, A.; Barbiroli, B. *Biochim. Biophys. Acta*−Bioenerg. **2005**, *1708*, 164−177.
(8) Romani, A.; Maguire, M. *Biometals* **2002**, *3*, 271−283.
(9) Iotti, S.; Gottardi, G.; Barbiroli, B. In *Proceedings of the International Society for Magnetic Resonance in Medicine*, 6th Scientific Meeting, Sydney, Australia, 1998; p 1796.
(10) (a) Bond, M.; Vadasz, G.; Somlyo, A. V.; Somlyo, A. P. *J. Biol. Chem.* **1987**, *262*, 15630−15636. (b) Di Francesco, A.; Desnoyer, R. W.; Covacci, V.; Wolf, F. I.; Romani, A.; Cittadini, A.; Bond, M. *Arch. Biochem. Biophys* **1998**, *360*, 149−157.
(11) *The Handbook*−A Guide to Fluorescent Probes and Labeling Technologies, 10th ed,; Haugland, R. P., Ed.; Molecular Probes: Eugene, OR, 2005.
(12) (a) Fatholahi, M.; LaNoue, K.; Romani, A.; Scarpa, A. *Arch. Biochem. Biophys.* **2000**, *374*, 395−401. (b) Wolf, F. I.; Covacci, V.; Bruzzese, N.; Di Francesco, A.; Sacchetti, A.; Corda, D.; Cittadini, A. *J. Cell. Biochem.* **1998**, *71*, 441−448.
(13) (a) Komatsu, H.; Iwasawa, N.; Citterio, D.; Suzuki, Y.; Kubota, T.; Tokuno, K.; Kitamura, Y.; Oka, K.; Suzuki, K. *J. Am. Chem. Soc.* **2004**, *126*, 16353−16360. (b) Kubota, T.; Shindo, Y.; Tokuno, K.; Komatsu, H.; Ogawa, H.; Kudo, S.; Kitamura, Y.; Suzuki, K.; Oka, K. *Biochim. Biophys. Acta* **2005**, *1744*, 19−28. (c) Komatsu, H.; Miki, T.; Citterio, D.; Kubota, T.; Shindo, Y.; Kitamura, Y.; Oka, K.; Suzuki, K. *J. Am. Chem. Soc.* **2005**, *127*, 10798−99.
(14) Bordunov, A. V.; Bradshaw, J. S.; Zhang, X. X.; Dalley, N. K.; Kou, X.; Izatt, R. M. *Inorg. Chem.* **1996**, *35*, 7229−7240.
(15) Prodi, L.; Bolletta, F.; Montalti, M.; Zaccheroni, N.; Savage, P. B.; Bradshaw, J. S.; Izatt, R. M. *Tetrahedron Lett.* **1998**, *39*, 5451−5454.

time-resolved anisotropy measurements were obtained with a modular UV−vis−NIR spectrofluorometer (Edinburgh Instruments), equipped with single-photon counting apparatus.

Titration of Mg^{2+} Binding by Fluorescence Spectroscopy. Aliquots of a $MgSO_4$ solution were added to a 25 μM solution of **1** or **2** in DPBS to give Mg^{2+} concentrations between 6 μM and 2 mM, and fluorescence spectra upon excitation at 363 nm were recorded. The measurements were performed in triplicate to ensure accuracy of the derived K_d value. The emission spectra were then integrated from 400 to 700 nm, and the obtained values were fitted[16] to $I = \phi_u C_u + \phi_c C_c$, where C_u and C_c are the concentrations of the uncomplexed and complexed probe, respectively, and ϕ_u and ϕ_c are the proportionality constants between the emission intensity (in arbitrary units) and the concentration of the uncomplexed and complexed probe, respectively. C_c satisfies the usual binding expression in eq 1, where M_{tot} is the total concentration of added metal ion:

$$C_c^2 - [(C_c + C_u) + M_{tot} + K_d]C_c + M_{tot}(C_u + C_c) = 0 \quad (1)$$

Cell Culture. HL60 (human promyelocytic leukemia cells) and HC11 (mouse mammary epithelial cells) were grown at 37 °C and 5% CO_2 in RPMI 1640 medium supplemented with 10% heat-inactivated fetal calf serum (FCS), 2 mM L-glutamine, 1000 units/mL penicillin, and 1 mg/mL streptomycin.

Total Cell Mg^{2+} Measurements. Total Mg^{2+} content by atomic absorption spectroscopy (AA) was assessed on acidic cellular extracts. To remove extracellular Mg^{2+} contamination, cultures were rapidly washed twice with cold PBS. Ion extraction was performed by adding 3 mL of 1.0 N HNO_3. Cell extracts were carefully collected and centrifuged, and Mg^{2+} was assayed on properly diluted supernatants by a Perkin-Elmer atomic absorption spectrometer, as previously described.[10b]

Fluorescence Measurements and Cell Imaging. For fluorescence spectroscopy, the cells were washed twice with DPBS, suspended at 5 $\times$ 10^5 cells/mL, and incubated with 25 μM fluorophore for 5 min. Homogenization was obtained by sonication of aliquots of cell samples, and fluorophores were added thereafter.

The cellular total Mg^{2+} was estimated according to

$$[\mathrm{Mg}] = \frac{k_d(F - F_{min})/(F_{max} - F_{min})}{1 - (F - F_{min})} + \{[\mathrm{dye}](F - F_{min})/(F_{max} - F_{min})\} \quad (2)$$

where F is the fluorescence intensity of the sample incubated with the fluorophore, F_{max} is the fluorescence intensity of the sample upon addition of saturating amount of $MgSO_4$ (final concentration 2 mM), and F_{min} is the fluorescence intensity of the sample upon addition of EDTA (final concentration 4 mM).

For confocal microscopy measurements HC11 cells were seeded (10^5/plate) on glass bottom dishes (0.17 mm cover glass, WillCo Wells) and grown for at least 24 h before experiments were performed. Cells were then washed twice in PBS, incubated with 25 μM fluorophore in PBS for 5 min at room temperature protected from light, and immediately placed on the stage of the microscope for imaging.

Imaging was performed by two-photon absorption (TPA) fluorescence. A conventional confocal laser-scanning microscope consisting of an inverted microscope (TE2000E, Nikon) and a C1 Nikon Plus scanning head was converted for TPA use.[17] TPA fluorescence was excited by a Ti:sapphire ultrafast laser source (Mai Tai Laser 750−850, Spectra Physics, CA) set at wavelength 750 nm and output power 850 mW, which corresponds to approximately 6 mW of average power in the focal plane. The fluorescence signal, collected by the objective (Plan Apochromat 60X/1.40/0.21/Oil, Nikon, Florence, Italy) and selected by a filter (HQ535-50, Chroma Inc., Brattleboro, VT), was fed to a multimode fiber directed to a photomultiplier (R928, Hamamatsu, Milan, Italy) in the C1 plus controller.

Image acquisition was performed with residence times ranging from 1.4 to 4.5 μs/pixel and open pinhole. Acquired images were analyzed with Image J 1.33, the open source software by NIH (Bethesda, MD). Fluorescence increment was expressed as the pseudoratio

$$\Delta F/F = (F - F_{base})/(F_{base} - B)$$

where F is the measured fluorescence intensity of the probe, F_{base} is the mean fluorescence intensity of the probe in the cell before stimulation, and B is the background signal determined from the average of three areas adjacent to the cell.

Results and Discussion

Photophysical Properties of the Probes. The absorption and fluorescence bands of the probes **1** and **2** are mainly due to the presence in their structure of 8-hydroxyquinoline (HQ) derivatives, whose photophysical properties have been extensively studied.[18] Figure 2 reports the absorption spectra of compounds **1** and **2** in DPBS, which share a similar shape: a very intense band lies in the 230−250 nm region, which has been attributed to a $\pi-\pi^*$ transition, while a less intense and broader nonstructured band lies at lower energy (360 nm). As previously reported,[19] this band is associated with a transition in which substantial charge density is transferred from the oxygen atom to the quinoline moiety of the chromophore. In their fluorescence spectra, hydroxyquinoline derivatives present a nonstructured fluorescence band in the 360−520 nm region, whose intensity and energy are strongly affected by the nature of the solvent. In general, HQ derivatives are, however, poorly luminescent, due to an intermolecular photoinduced proton transfer (PPT) process between the hydroxyl group (which is a relatively strong photoacid) and the nearby quinoline nitrogen (which is, in turn, a strong photo base). In addition, in protic media, intermolecular PPT processes involving solvent molecules can also occur, further decreasing the fluorescence quantum yield of this kind of fluorophore.

The absorption and fluorescence bands of both **1** and **2** in DPBS dramatically change upon addition of Mg^{2+} ions, a behavior previously observed for **2** in MeOH/H_2O (1/1) solution.[15] In the case of probe **2**, the UV band is red-shifted to 260 nm, while the low-energy transition band is strongly shifted to the 300−400 nm region. The shift of this band can also be observed for **1**, while a less marked shift, accompanied by a broadening of the band, is observed for the higher energy transition. These findings are characteristic of the HQ derivatives when a complexation process is accompanied by the deprotonation of the hydroxyl group and indicate that also in DPBS

(16) Prodi, L.; Bolletta, F.; Zaccheroni, N.; Watt, C. I.; Mooney, N. J. *Chem. Eur. J.* **1998**, *4*, 1090−1094.
(17) Ridsdale, A.; Micu, I.; Stys, P. K. *Appl. Opt.* **2004**, *43*, 1669−1675.
(18) (a) Bardez, E.; Devol, I.; Larrey, B.; Valeur, B. *J. Phys. Chem. B* **1997**, *101*, 7786−7793. (b) Goldman, M.; Wehry, E. L. *Anal. Chem.* **1970**, *42*, 1178−1185. (c) Prodi, L.; Bargossi, C.; Montalti, M.; Zaccheroni, N.; Su, N.; Bradshaw, J. S.; Izatt, R. M.; Savage, P. B. *J. Am. Chem. Soc.* **2000**, *122*, 6769−6770. (d) Prodi, L.; Montalti, M.; Zaccheroni, N.; Bradshaw, J. S.; Izatt, R. M.; Savage, P. B. *Tetrahedron Lett.* **2001**, *42*, 2941−2944. (e) Prodi, L.; Montalti, M.; Bradshaw, J. S.; Izatt, R. M.; Savage, P. B. *J. Inclusion Phenom. Macrocyclic Chem.* **2001**, *41*, 123−127. (f) Casnati, A.; Sansone, F.; Sartori, A.; Prodi, L.; Montalti, M.; Zaccheroni, N.; Ugozzoli, F.; Ungaro, R. *Eur. J. Org. Chem.* **2003**, 1475−1485. (g) Bronson, R. T.; Montalti, M.; Prodi, L.; Zaccheroni, N.; Lamb, R. D.; Dalley, N. K.; Izatt, R. M.; Bradshaw, J. S.; Savage, P. B. *Tetrahedron* **2004**, *60*, 11139−11144.
(19) (a) Ballardini, R.; Varani, G.; Indelli, M. T.; Scandola, F. *Inorg. Chem.* **1986**, *25*, 3858−3865. (b) Ballard, R. E.; Edwards, J. W. *J. Chem. Soc.* **1964**, 4868−4874.

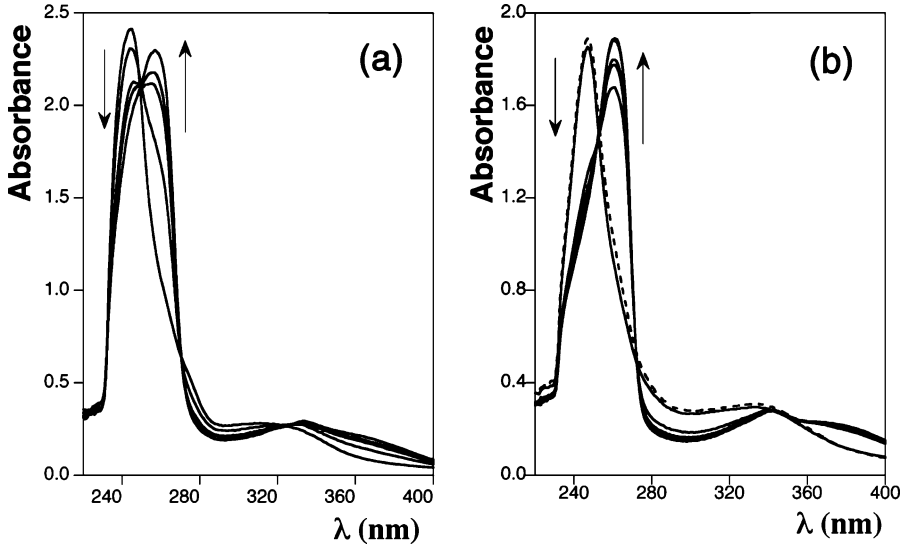

Figure 2. Absorption spectra of probes **1** (a) and **2** (b) (25 μM) in DPBS at room temperature and upon addition of increasing amounts of Mg^{2+} ions (0, 40, 250, 500, 800, and 5000 μM).

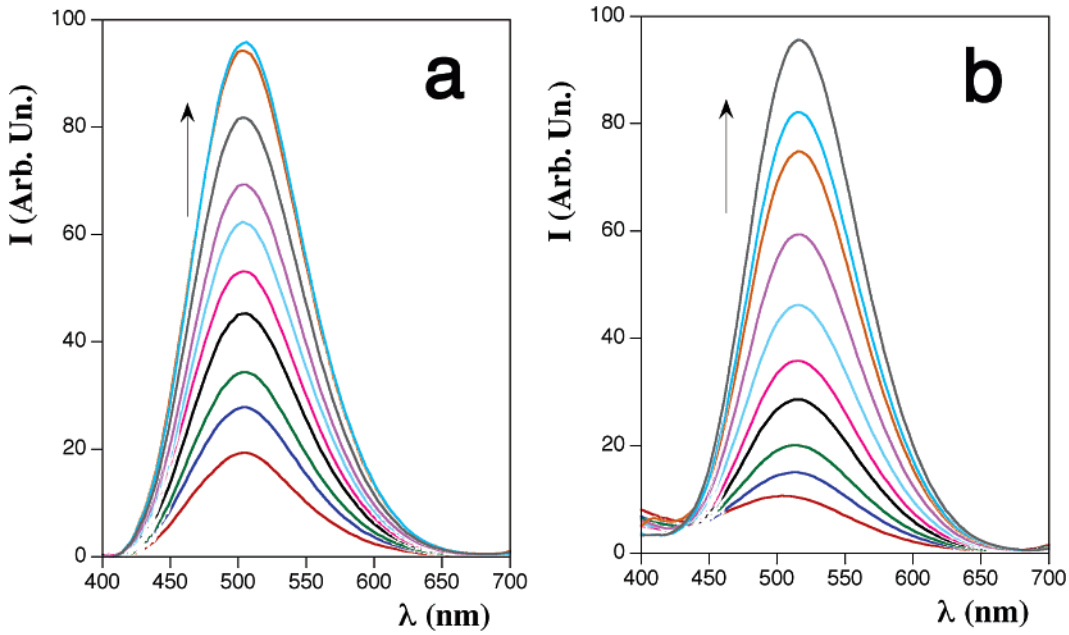

Figure 3. Fluorescence spectra (λ_{ex} = 363 nm) of probes **1** (a) and **2** (b) (25 μM) in DPBS at room temperature upon addition of increasing amounts of Mg^{2+} ions (0, 5, 10, 30, 50, 87, 280, 480, 850, and 1030 μM).

the probes **1** and **2** are able to bind magnesium ions with high affinity. The presence of three different, clear isosbestic points for both probes supports the formation of a complex with only one stoichiometry.

Figure 3a reports the emission spectra of probe **1** at different Mg^{2+} concentrations. A dramatic enhancement of the fluorescence is observed at increasing Mg^{2+} concentrations; similar results were also obtained with probe **2** (Figure 3b). The remarkable increase of the fluorescence intensity is due to the fact that both PPT and photoinduced electron transfer (PET) processes are inhibited in the fluorescent complex. It has been demonstrated that tertiary amines close to HQ derivatives, as in the case of **1** and **2**, are able to quench the fluorescence quantum yield because of PET processes from the amine to the HQ moiety.[18f,g] In the Mg^{2+} complexes of **1** and **2**, the PPT and PET processes are not active because the amino group of the macrocyclic ring acts as a general base and serves to deprotonate the 8-HQ hydroxyl group. Thus, the PPT processes are precluded because the HQ hydroxyl groups are deprotonated, and the PET processes are not possible because the proximal amine groups are protonated (tying up the lone pairs of electrons responsible for the PET processes).

The excitation spectra of the **1** and **2** complexes with Mg^{2+}, recorded in the region between 450 and 600 nm, are almost superimposable with their absorption spectra (not shown). The fluorescence lifetimes of **1** and **2**, in DPBS solutions at pH 7.0, are 7.1 and 4.6 ns, respectively. Notably, both values are considerably shorter than the corresponding ones observed in MeOH/DPBS 1/1 (16.6 and 17.9 ns, respectively). Since the observed fluorescence is associated with a charge-transfer transition in which substantial charge density is transferred from the oxygen atom to the quinoline moiety, a dependence of lifetime on solvent polarity is not unexpected, as already observed for other chromophores.[20]

As to the affinity of probes **1** and **2** for Mg^{2+}, K_d values of 44 ± 5 and 73 ± 4 μM, respectively, were calculated from the fluorescence spectra obtained by titrating the compounds with $MgSO_4$ in DPBS (Figure 4 for probe **2**). It is important to note that probes **1** and **2** have a much stronger affinity for Mg^{2+} ions than other available Mg^{2+} probes, as fura-derived indicators and KMGs have K_ds between 2 and 4 mM.[11,13] This feature is important for practical applications and suggests that probes **1** and **2** can be exploited for assessing total content of Mg^{2+} in living cells.

The fluorescence response of probe **1** and **2** is highly selective for Mg^{2+}: alkali metal ions in the 100 mM range do not affect the fluorescence intensity of the probes, nor do they induce any change on the intensity of their magnesium complexes, which indicates that these metal ions do not interfere with Mg^{2+} detection (data not shown). Ca^{2+} concentrations as high as 10 mM (much higher than the typical intracellular concentration) produce only a very small increase in fluorescence intensity of the probe alone and a small decrease of the fluorescence intensity of its complexes with Mg^{2+} (see Figure 5 for probe **2**). Other alkaline earth metal ions show the same behavior as described for the alkali metal ions. First-row transition metal ions including Mn^{2+} quench fluorescence, with the noticeable exception of Zn^{2+}, which induces an increase in the fluorescence intensity, although considerably lower than that observed upon addition of Mg^{2+} (not shown). Moreover, the affinity of these probes is lower for Zn^{2+} than for Mg^{2+}. For example, the K_d of the complex of probe **2** with Zn^{2+} in methanol is 50-fold higher than that with Mg^{2+} (7.6 vs 0.15 μM, respectively).[14] When the large difference in the intracellular concentrations of Zn^{2+} and Mg^{2+} is also taken into account,[21] these results clearly indicate that the former does not cause substantial interference in Mg^{2+} determination.

Since the two probes contain multiple acidic and basic sites, and considering that the complexation process requires the deprotonation of the hydroxyl groups, it is of great importance to evaluate whether the fluorescence of the complex can be affected by changes in pH within the physiological range. In particular, we observed (Figure 6) that, in the presence of an excess of Mg^{2+} ions, the fluorescence of probe **2** was constant at pH ranging between 6.3 and 7.5 and decreased at lower or higher pH values, while the fluorescence of probe **1** increased gradually up to pH 7, reaching a plateau between pH 7.0 and 7.6.

Photochemical Properties of Probes 1 and 2 in Cell Environments. When probes **1** and **2** are added to cell suspensions (HL60 and HC11) incubated in Mg-free medium, clear-cut fluorescence emission spectra can be detected, indicating that the probes are accessible to intracellular Mg^{2+}. For **1**, the emission bands do not undergo shifts larger than 5 nm with respect to those detected in DPBS, and the same holds true for the excitation spectra (not shown). In the case of **2**, instead, a larger red shift (ca, 20 nm) can be observed. Noteworthy for both the cell lines examined, fluorescence decay can be conveniently fitted only if two different excited-state lifetimes are considered (see Table 1). It is important to note that the two observed lifetimes are very similar for both cell lines. The two different families of excited-state lifetimes indicate that the probes are surrounded by two different environments, a more polar one that is likely the cytosol, which gives τ_1, and a less polar one when the probes are localized, for example in membranes, which gives τ_2. This interpretation is supported by two results: first, the increase in the excited-state lifetimes observed in MeOH/DPBS (1/1) in comparison to those in DPBS, as outlined above; second, the observation that, upon cell breakage by sonication, the two observed lifetimes do not substantially change, while the weight of the preexponential term of the longer component decreases about 10-fold.

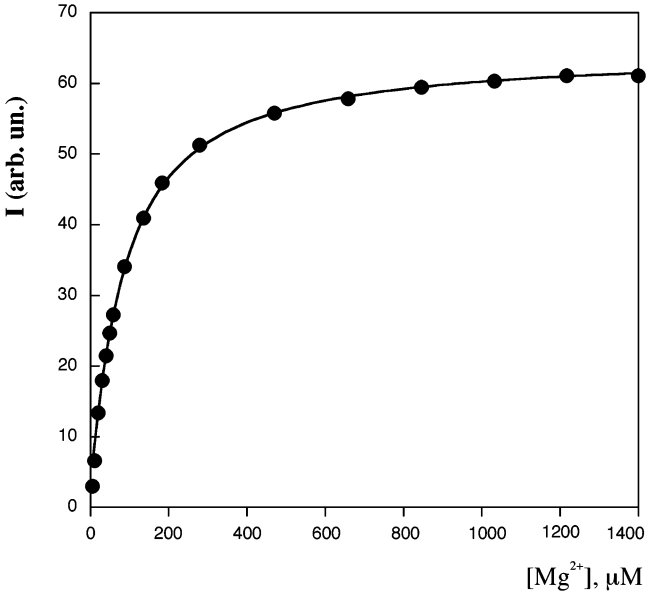

Figure 4. Fluorescence titration of probe **2** with Mg^{2+} (λ_{ex} = 363 nm, emission intensity integrated in the 400−700 nm region).

Another interesting point is related to the presence of a fluorescence anisotropy of 0.08 observed when the probes are inside the cell, while, as expected, the anisotropy is not observed when the probes are in DPBS. This finding can be ascribed to the immobilization of part of the dyes inside membranes and organelles.

Such characteristics are particularly appealing, as they might appropriately be harnessed to get information on local environment and ion compartmentalization by innovative imaging techniques, such as fluorescence lifetime imaging (FLIM), which is independent of fluorophore concentration, fluorescence intensity, light path length, and photobleaching.[22]

Probes 1 and 2 in the Study of Cellular Mg^{2+} Homeostasis.: (A) Assessment of Total Cell Magnesium. As discussed in the Introduction, bound and free Mg^{2+} pools play an important and interconnected role in cell Mg^{2+} homeostasis. Therefore, the availability of an additional fluorescent probe able to detect total cell Mg^{2+} appears very attractive. We investigated the possibility that probes **1** and **2** could be used to assess total cell Mg^{2+}, as the low K_ds of these fluorophores would suggest. To this end we compared data obtained by AA to those derived from fluorescence spectroscopy of probe **1** in different cell lines. In HL60 leukemia cells, fluorescence data fitted according to eq 2 provided a nearly 4-fold overestimation of total Mg^{2+} values obtained by AA (41.2 ± 17.1 vs 11.9 ± 1.5 nmol/10^6 cells, respectively). Interestingly, a comparable

(20) Prodi, L.; Montalti, M.; Zaccheroni, N.; Dallavalle, F.; Folesani, G.; Lanfranchi, M.; Corradini, R.; Pagliari, S.; Marchelli, R. *Helv. Chim. Acta* **2001**, *84*, 690−706.
(21) Williams, R. J. P.; Frausto da Silva, J. J. R. *Coord. Chem. Rev.* **2000**, *200−202*, 247−348.
(22) Tadrous, P. J. *J. Pathol.* **2000**, *191*, 229−234.

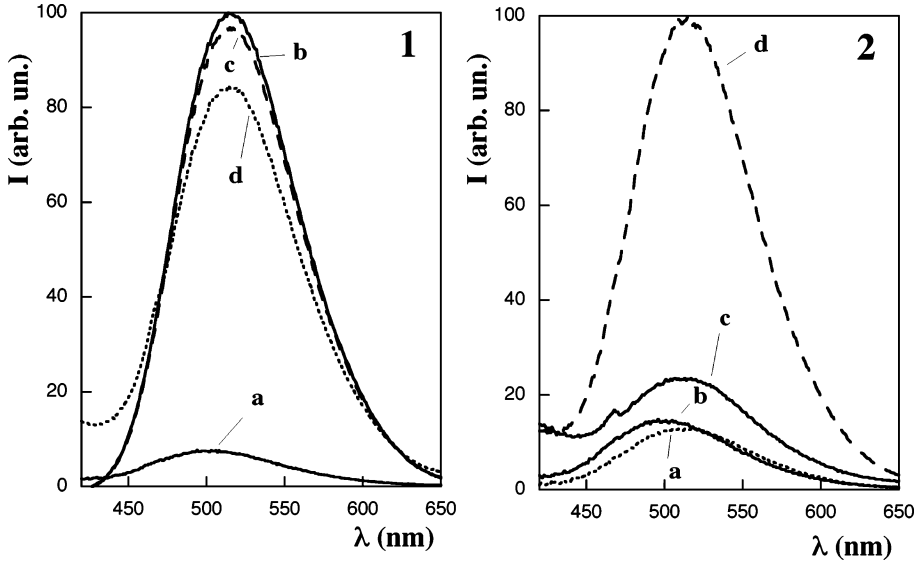

Figure 5. Effect of sequential addition of Ca^{2+} and Mg^{2+} and vice versa on fluorescence spectra (λ_{ex} = 363 nm) of probe **2** in DPBS at room temperature. (Panel 1) Probe **2** (25 μM) (a), plus Mg^{2+} 350 μM (b), plus Ca^{2+} (200 μM) (c), plus Ca^{2+} 2 mM (d). (Panel 2) Probe **2** (25 μM) (a), plus Ca^{2+} 350 μM (b), plus Ca^{2+} 2 mM (c), plus Mg^{2+} (2.0 mM) (d).

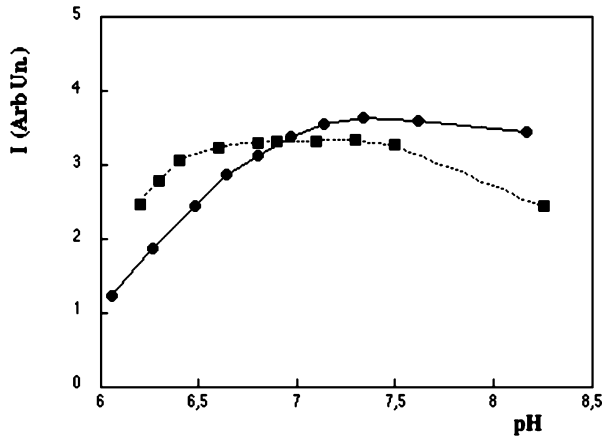

Figure 6. pH dependence of the fluorescence intensity (λ_{ex} = 363 nm, λ_{em} = 500 nm) of probes **1** (●) and **2** (■) in DPBS in the presence of Mg^{2+} (2 mM).

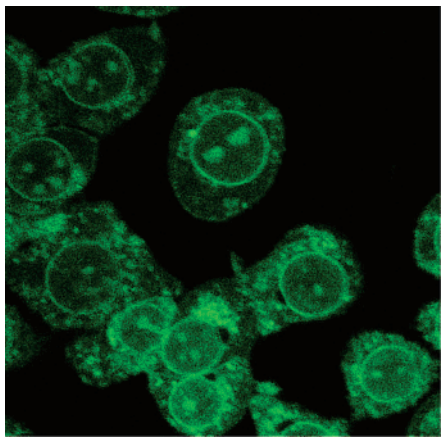

Figure 7. Probe **1** distribution in HC11 mouse mammary cells. Cells were loaded with probe **1** (25 μM) and imaged by two-photon fluorescence microscopy (λ_{ex} = 750 nm), as detailed in the Experimental Section.

Table 1: Excited-State Lifetimes of Probes **1** and **2** inside Different Cells

	probe **1**		probe **2**	
	τ_1 (ns)	τ_2 (ns)	τ_1 (ns)	τ_2 (ns)
HC11	8.5	26.0	8.3	24.0
HL60	11.7	27.7	6.6	21.4

overestimation was also obtained in HC11 epithelial cells. These results are not wholly unexpected because eq 2 does not take into account (a) the longer excited-state lifetimes (and as a consequence, the more intense fluorescence quantum yields) found in whole cells with respect to pure DPBS and (b) the potentially different distribution of the probes inside and outside the cells. Indeed, when HL60 cells were disrupted by sonication, producing a near-homogeneous suspension, eq 2 gave a magnesium concentration of 11.4 ± 4 nmol/10^6 cells, in very good agreement with AA measurements. These results suggest that use of chemosensors **1** and **2** provides a new straightforward analytical method for the detection of cell total magnesium.

(B) Mapping Intracellular Mg^{2+} Distribution and Movements by Confocal Imaging. The advantageous photochemical properties of probes **1** and **2** were also exploited to investigate Mg^{2+} intracellular distribution and kinetics by 3D confocal imaging. Excitation of the probes in the UV region was achieved by quasi-simultaneous absorption of two photons of approximately double the required wavelength (750 nm). Two-photon excitation allows the same or higher depth resolution of conventional confocal microscopy but minimizes fluorophore bleaching and photodamage to the cells, consequently prolonging the maximal observation time.

Probes **1** and **2** are readily taken up into cells: a 5-min incubation at room temperature is sufficient to detect a significant increase in cell-bound fluorescence, which persists for up to 1 h and can be turned off in about 2−5 min by addition of 0.1 mM EDTA (not shown). As shown by Figure 7, fluorescence appears to be localized diffusely over the cytosol. More precisely, optical sectioning on the *z* plane evidenced reinforcements of the fluorescence signal in the perinuclear area and in nuclear regions resembling nucleoli (Figure 7).

Such localization is consistent with the subcellular distribution of Mg^{2+} measured by conventional techniques, which indicate that the largest portions of the ion occur within the microsomal

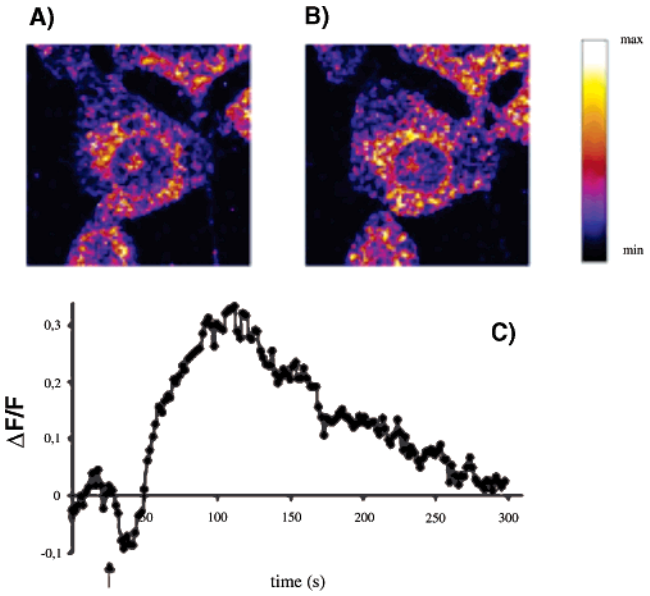

Figure 8. Pseudocolored images of HC11 cells loaded with probe **1** (25 μM), before (A, $t = 0$ s) and after (B, $t = 110$ s) treatment with FCCP (5 μM). (C) Time course of fluorescence increment upon FCCP addition (arrow, $t = 30$ s), expressed as $\Delta F/F = (F - F_{base})/(F_{base} - B)$ as detailed in the Experimental Section. Results are shown as single-cell response in a representative experiment.

and mitochondrial fractions of the cell.[3,10] Moreover, the strong affinity of Mg^{2+} for ATP and RNA further supports the specificity of the staining pattern shown in the figure. Intracellular Mg^{2+} stores remain to be characterized by appropriate colocalization studies.

We also demonstrated that probe **1** can be a valuable tool for dynamic measurements of Mg^{2+} distribution and mobilization. Carbonyl cyanide *p*-trifluoromethoxyphenylhydrazone (FCCP) is a mitochondrial uncoupler, which abolishes the linkage between electron transport and oxidative phosphorylation, destroying mitochondrial membrane potential and leading to ion fluxes. Figure 8 shows that, in HC11 cells, addition of FCCP elicited a transient increase of probe **1** fluorescence, indicative of an intracellular Mg^{2+} redistribution. This observation is in agreement with Mg^{2+} fluctuation described in PC12 cells loaded with the new dye KMG104.[13b,c] Ongoing research will provide information on the observed intracellular Mg^{2+} transient.

Conclusions

We have shown the photochemical characterization and application in live cell imaging of the DCHQ chemosensors **1** and **2**. The binding of these probes to Mg^{2+} is very sensitive, is highly selective for the cation, is not affected by pH changes in the physiological range, and displays much higher affinity than other available probes for Mg^{2+}. Probes **1** and **2** are readily permeable to cells and, due to their K_d values in the micromolar range, are promising tools to assess total cell Mg^{2+} in living cells, giving information that can be complementary to that obtained with recently described probes.[13]

In particular, fluorescence measurements of probe **1** in sonicated cells are in good agreement with AA data, indicating that the described approach is a good platform for the development of a new, straightforward, and sensitive analytical method for the determination of cell total Mg^{2+}. Furthermore, 3D imaging by confocal microscopy of cells loaded with probes **1** and **2** also suggests that these compounds are suitable to detect intracellular Mg^{2+} distribution and real-time movements of this cation. We therefore believe that this class of fluorophores and their derivatives might be exploited as novel specific, sensitive, and effective fluorescent sensors for intracellular Mg^{2+} ion, contributing to shed new light on magnesium homeostasis at the cellular level.

Acknowledgment. We thank Professor Matteo A. Russo from Università di Roma La Sapienza for the use of the two photon confocal microscope and Dr Luisa Stella Dolci and Dr Matteo Simonacci for contributing to experimental work. Financial support from MIUR (FISR-SAIA and FIRB-LATEMAR to L.P., PRIN 2003067599 to F.I.W. and 2004058357 to S.I.) is gratefully acknowledged.

JA056523U